

Received: 2017.09.12

Accepted: 2018.01.03

Published: 2018.06.11

Tail Vein Infusion of Adipose-Derived Mesenchymal Stem Cell Alleviated Inflammatory Response and Improved Blood Brain Barrier Condition by Suppressing Endoplasmic Reticulum Stress in a Middle Cerebral Artery Occlusion Rat Model

Authors' Contribution:
Study Design A
Data Collection B
Statistical Analysis C
Data Interpretation D
Manuscript Preparation E
Literature Search F
Funds Collection G

ABE **Lumei Chi**
BC **Yujing Huang**
BC **Ying Mao**
B **Kunjun Wu**
BE **Li Zhang**
A **Guangxian Nan**

Department of Neurology, China-Japan Union Hospital of Jilin University, Changchun, Jilin, P.R. China

Corresponding Author: Guangxian Nan, e-mail: nanguangdhhd@163.com
Source of support: Departmental sources

Background: The current study was designed to explore the pathway through which adipose-derived mesenchymal stem cells (ADMSCs) affect brain ischemic injury.





Material/Methods: The improving effect of ADMSCs on the brain function and structure was evaluated in a middle cerebral artery occlusion (MCAO) rat model. The permeability of the brain-blood barrier (BBB), inflammatory response, and endoplasmic reticulum (ER) stress-related signaling induced by ischemia were determined.

Results: The administration of ADMSCs decreased neurological severity score when compared with that in the MCAO group and also restricted the brain infarction area as well as cell apoptosis. ADMSCs suppressed the inflammation in brains by decreasing the expressions of IL-1 β , IL-6, and TNF- α , contributing to the decreased permeability of the BBB. The expressions of pro-apoptosis factors in ER stress were inhibited while that of anti-apoptosis factors were induced.

Conclusions: ADMSCs affected brain injury in multiple ways, not only by suppressing inflammation in the brain infarction area, but also by blocking ER stress-induced apoptosis.

MeSH Keywords: **Blood-Brain Barrier • Endoplasmic Reticulum Stress • Infarction, Middle Cerebral Artery • Inflammation • Mesenchymal Stromal Cells**

Full-text PDF: <https://www.medscimonit.com/abstract/index/idArt/907096>

 3399  3  5  30



Background

Ischemic stroke (IS) ranks third in causes of mortality in industrialized countries and is the leading cause of long-term disability worldwide [1,2]. Characterized by thromboembolic vascular occlusion and a strong inflammatory response, IS has an annual incidence rate of approximately 250–400 in 100 000 population [3,4]. Few approaches besides thrombolytic treatments are currently available for treating impairments due to IS. However, hampered by a narrow time window [5,6] and severe hemorrhagic complications, thrombolytic therapies are limited [7]. Thus, there is an urgent need for development of safe and effective alternative treatments for IS patients who are not suitable for thrombolytic therapy.

Cerebral ischemia induces a dramatic activation and release of cytokines, chemokines, and adhesion molecules [8]. Unlike the function pattern between the blood and nervous system, inflammatory mediators released in the area of IS can modulate permeability of the blood–brain barrier (BBB) [9,10]. Once the BBB is impaired, leukocytes readily move into brain tissues [11] and further exacerbate brain damage [9]. Therefore, the modulation of inflammation is a promising therapeutic avenue for treating IS. Recent clinical trials have proven the feasibility and safety of stem cell-based therapies for IS [3]. Stem cells can be classified into embryonic stem cells (ESCs) and adult stem cells (ASCs), both of which have the potential to develop into a variety of differentiated cells [12,13]. But in contrast to the pluripotency of ESCs, ASCs are generally found within tissues and give rise to certain types of cells, including mesenchymal stem cells (MSCs) [12,14]. MSCs derived from bone marrow (bone marrow mesenchymal stem cells, BMSCs) have been comprehensively studied for treatment of IS [15,16]. However, due to the invasive method used to obtain them, clinical use of BMSCs is difficult. Compared with ESCs and BMSCs, adipose-derived mesenchymal stem cells (ADMSCs) are abundant and easy to obtain without serious invasiveness and ethical issues [17]. A previous report has also confirmed the therapeutic superiority of ADMSCs over BMSCs in a liver injury animal model [18]. The effectiveness of ADMSCs in treating IS was demonstrated in a middle cerebral artery occlusion (MCAO) rat model [17]. The modulating effect of human MSCs on endoplasmic reticulum (ER) stress was also validated in an MCAO rat model [19], strongly suggesting that treatment with MSCs alters inflammatory responses during an IS attack.

In the present study, an MCAO rat model was used to determine if ADMSCs can alleviate the damage caused by IS. By detecting the expressions of indicators involved in the inflammatory response, the permeability of the BBB, and ER stress, our study attempted to explain the mechanism through which ADMSCs alleviate IS damage.

Material and Methods

Chemicals

Detailed data on the antibodies used in the current study are listed in Supplementary Table 1.

Animals

Adult male Sprague-Dawley (SD) rats (weighing 200–300 g) were purchased from Changsheng Biotechnology Inc. (Benxi, Liaoning, China) and maintained in cages at room temperature (20–25°C) with a constant humidity (55±5%) and free access to food and water. All the procedures with animals were conducted in accordance with the Institutional Animal Ethics Committee and the Animal Care Guidelines of Jilin University.

Isolation of adipose-derived mesenchymal stem cells (ADMSCs) from rats

Rats were anesthetized using isoflurane, and adipose tissue surrounding the epididymis was carefully dissected and excised. After being washed with PBS 2 times, adipose tissues were cut into 1–2-mm³ pieces and placed into stock collagenase solution at a concentration of 0.5 units/ml. Then, the suspension was thoroughly mixed using a shaker (WD-9405B, Liuyi Factory, Beijing, China) and incubated with constant agitation at 37°C for 60 min. After incubation, the suspension was triturated with a pipette and filtered using a 70-µm nylon net. After being centrifuged at 157× g for 10 min, the precipitation was resuspended with PBS and centrifuged at 157× g for 10 min. Then, the cells were cultured in DMEM (SH30023.01B, Hyclone, Carlsbad, USA) at 37°C in an atmosphere consisting of 5% CO₂ and 95% air for 24 h. The suspension was then discarded and the remaining cells were used as ADMSCs.

Identification of ADMSCs

Osteogenic and adipogenic differentiation potential of the cells were assessed using Alizarin Red S and Oil Red O experiments following procedures published previously [20]. At 30 min before transplantation into model animals, the expressions of CD29, CD34, CD44, CD45, and CD90 on the cell surface were detected using flow cytometry (Accuri C6, BD, USA). Detailed information on antibodies is listed in Supplementary Table 1.

Induction of middle cerebral artery occlusion (MCAO) model and administration of ADMSCs

After culturing ADMSCs for 2 weeks, SD rats were subjected to induction of the MCAO model as follows. The left common carotid artery (LCCA) was exposed and a small incision was made on the LCCA. Then, the left middle cerebral artery (LMCA) was

occluded using a 0.28-mm nylon filament. One hour after occlusion, the nylon filament was removed and the muscle and skin were closed in layers. In total, 108 animals were randomly grouped into 3 groups (36 for each group): in the sham group, animals underwent standard procedures without occlusion using a nylon filament; in the MCAO group, animals were subjected to MCAO model induction; and in the MCAO+ADMSC group, rats received tail vein injection of $2.0 \times 10^6 / 0.5$ ml ADMSCs 3 times at 0, 12, and 24 h after MCAO model induction to ensure the sufficient function of the cells. According to the experimental design, 18 of the 36 rats were used for the BBB permeability assay (6 for each time point). The remaining 18 animals in different groups were raised under the same conditions for 2 weeks before being sacrificed for histological and molecular detection: 6 rats were used for triphenyltetrazolium (TTC) staining, 6 rats were used from TUNEL and immunofluorescent detection, and the remaining 6 rats were used for functional tests, reverse transcription real-time PCR (RT²-PCR), and Western blotting assays.

ADMSCs labeling

At 30 min before transplantation, CM-Dil (Vybrant™ Dil cell-labeling solution, Molecular Probes, Eugene, USA) (50 µg/ml) was added to the culture medium. Cells labeled by the dye are visible in a brain ischemic penumbra area due to the distinctive fluorescence of the dye. Results were detected with fluorescent microscopy (BX53, OLYMPUS, Tokyo, Japan).

Functional test

Behavioral tests for assessment of brain function of all animals were performed at 0, 1, 3, 7, and 14 days after model induction. The tests were performed using the Modified Neurological Severity Score (mNSS) by staff who were blind to the experiment designs, according to previous reports [21].

BBB permeability assay

At 0, 7, and 14 days after model induction, the BBB permeability was measured using Evans Blue dye method: briefly, 0.1 ml Evans Blue dye (2%) (314-13-6, Sigma, MO, USA) was intravenously injected into tail veins 5 h before rats were sacrificed. Then, brain samples were collected and homogenized with PBS. The homogenate was subjected to centrifugation at $15\ 000 \times g$ for 30 min. The supernatant was collected, mixed with the same volume of 50% trichloroacetic acid, and incubated at 4°C overnight. Afterwards, samples were centrifuged at $15\ 000 g$ for 30 min and the supernatant was collected. The OD value at 615 nm was measured with a Microplate Reader (ELX-800, BIOTEK, USA) to determine the amount of Evans Blue dye per gram brain tissue.

TTC staining and TUNEL staining

Two weeks after MCAO model induction, the remaining animals in different groups were killed and brain tissues were collected. Then, the infarction area in the whole-brain tissues were determined using 2,3,5-triphenyltetrazolium chloride (TTC) (298-96-4, Solarbio, Beijing, China) method. Briefly, brain tissues were cut into 2-mm slices and then incubated in 1% TTC for 10 min at 37°C to allow the demarcation of the infarcted region; the infarcted area was pale. The percentages of infarcted area in each slice were measured using the Image-Pro Plus software (Media Cybernetics, Bethesda, MD, USA); the percentage of infarcted area = infarcted area (mm²) / total area (mm²) × 100%. Cell apoptotic rates in ischemic penumbra part of brain tissues were also determined using an In Situ Cell Death Detection Kit (11684817910, Roche, Switzerland) following the manufacturers' instructions.

Immunofluorescent assay

Ischemic penumbra parts of brain tissues were first fixed with 4% paraformaldehyde for 15 min and then incubated with 0.1% Triton X-100 for 30 min. Afterwards, the slides were blocked in 10% goat serum and incubated with primary antibodies against different indicators (Supplementary Table 1) overnight at 4°C. Next, cells were incubated with Cy3-labeled secondary antibody (Supplementary Table 1) for 1 h in the dark, and then stained with 4,6-diamino-2-phenyl indole (DAPI) for 5 min at room temperature. Results were detected by fluorescent microscopy (BX53, OLYMPUS, Tokyo, Japan) at 400× magnification.

RT²-PCR

Total RNAs in ischemic penumbra part of brain tissues was extracted using the RNA Purified Total RNA Extraction Kit (RP1201, BioTek, Beijing, China). cDNA templates were achieved by reversely transcribing the RNA using Super M-MLV reverse transcriptase (RP6502, BioTek, Beijing, China). The reaction mixture contained 10 µl of 2×Power Taq PCR MasterMix (PR1702, BioTek, Beijing, China), 0.5 µl of each primer (IL-1β, forward: 5'-GCAATGGTCGGGACATAGTT-3', backward: 5'-CAGAGGACAGGG AGGAAA-3'. IL-6, forward: 5'-AACTCCATCTGCCCTTCA-3', backward: 5'-CTGTTGTGGGTGG TATCTC-3'. TNF-α, forward: 5'-TGGCGTGTTCATCCGTCT-3', backward: 5'-CCACTACTTCAGCGTCTCGT-3'. β-actin, forward: 5'-GGAGATTACTGCCCTGGCTCCTAGC-3', backward: 5'-GGCCGGACTCATCGTACTCCTGCTT-3'), 1 µl of the cDNA template, and 8 µl of RNase-free H₂O. Amplification was performed following a denaturation step at 95°C for 10 min, and then 40 cycles at 95°C for 10 s, 60°C for 20 s, and 72°C for 30 s, and stopped by 25°C for 5 min. Relative expression levels were calculated with Exicycler™ 96 (BIONEER, Daejeon, Republic Korea) according to the expression of 2^{-ΔΔCt}.

Western blotting assay

Total protein product in ischemic penumbra brain tissues was extracted using the Total Protein Extraction Kit (WLA019, Wanleibio, Shenyang, China). Concentrations of protein were determined using the BCA method. Then, 40 µg of protein was subject to 10% sodium dodecylsulfate polyacrylamide gel electrophoresis (SDS-PAGE). Primary antibodies against targeted proteins (Supplementary Table 1) were incubated with membranes at 4°C overnight. Next, secondary HRP IgG antibodies (1: 5000) were incubated with the membranes for 45 min at 37°C. The blots were developed using Beyo ECL Plus reagent (E002-5, 7seaBiotech, Shanghai, China). The results were recorded in the Gel Imaging System and analyzed with Gel-Pro Analyzer (Media Cybernetics, USA).

Statistical analysis

All data are expressed in the form of mean ± standard deviation. The difference between the MCAO and the MCAO+ADMSC groups was analyzed with the *t* test. The overall effect of ADMSCs was analyzed using ANOVA for repeated measurements. Statistical significance was accepted when *P* value (2-tailed) was smaller than 0.05. All analyses were conducted using SPSS version 19.0 (IBM, Armonk, NY, USA).

Results

Isolation and identification of ADMSCs

By using flow cytometry method, the third-passage ADMSCs expressed CD29, CD40, and CD90, but were negative for expression of CD34 and CD45, which are typical surface antibody feature of ADMSCs (Figure 1A). Moreover, the differentiation of ADMSCs toward osteogenic and adipogenic lineages was detected. The deposition of Alizarin Red could be observed for ADMSCs while adipose cells negatively reacted with Alizarin Red, representing the osteogenic differentiation potential of ADMSCs (Figure 1B). Similarly, the results of Oil Red O assays showed that the deposition of Oil Red O was observed only with ADMSCs (Figure 1C). The above results indicated the successful generation of ADMSCs in the present study.

Administration of ADMSCs improved the brain function of MCAO animals

Six rats in each group were subjected to mNSS testing 5 times: at 0, 1, 3, 7, and 14 days. The overall effect of ADMSCs on functional recovery of the brain was significant for rats who were administrated ADMSCs (Figure 2A; Supplementary Table 2) ($P<0.05$). For each single recording time point, the significant difference in mNSS could be detected starting at 7 days after

MCAO model induction (Figure 2A; Supplementary Table 2) ($P<0.01$). Although the treatment could not completely restore the brain function of MCAO rats when compared with the Sham group, ADMSCs did show potential as an alternative therapy to alleviate the impairments caused by brain ischemia.

Administration of ADMSCs suppressed apoptosis and decreased brain infarction area in ischemia brain tissues

The effect of ADMSCs in improving brain function was closely related to its function in brain cells. Results of TUNEL staining showed a suppressed proportion of apoptosis cells (stained brown) in brains tissues after administration of ADMSCs ($43.8\pm 10.9\%$ for the MCAO group vs. $29.3\pm 6.1\%$ for the ADMSC group), and the difference between the MCAO and the MCAO+ADMSC groups was statistically significant (Figure 2B) ($P<0.01$). After the administration of ADMSCs, the average infarction area in brain tissues was dramatically reduced: $19.8\pm 3.6\%$ in the MCAO group vs. $12.4\pm 2.6\%$ in the MCAO+ADMSCs group (Figure 2C) ($P<0.01$). Additionally, immunofluorescence staining (Figure 2D) identified CM-Dil-stained ADMSCs in the ischemic penumbra area of the MCAO rats, indicating the migration of ADMSCs to brain infarcted area after the injection.

Administration of ADMSCs improved BBB and suppressed inflammatory response in brain tissues of MCAO rats

The permeability of the BBB was evaluated with Evans Blue dye method. The induction of ischemia in rat brains increased the permeability of BBB. Although even without treatment, the BBB level would gradual decrease to a relatively normal level, administration of ADMSC accelerated the recovery process. As shown in Figure 3A and Supplementary Table 3, the difference at 7 days was statistically significant between the MCAO and the MCAO+ADMSCs groups ($P<0.01$). Furthermore, indicators representing the permeability of BBB, including OX-42, ZO-1, and Claudin-5, were also detected with immunofluorescent assay: the results illustrated that the administration of ADMSCs decreased the expression and distribution of OX-42 and increased the distribution of ZO-1 and Claudin-5 (Figure 3B–3D; Supplementary Figure 1) ($P<0.01$), representing the improved BBB condition. The BBB permeability of the MCAO rats was evidently improved by the injection of ADMSCs. Additionally, the expressions of the 3 pro-inflammation factors, including IL-1β, IL-6, and TNF-α, were inhibited by ADMSCs administration when compared with those in the MCAO group (Figure 4) ($P<0.01$). Our results suggest that the beneficial effects of ADMSCs on apoptosis and ischemic brain tissues occur through multiple mechanisms.

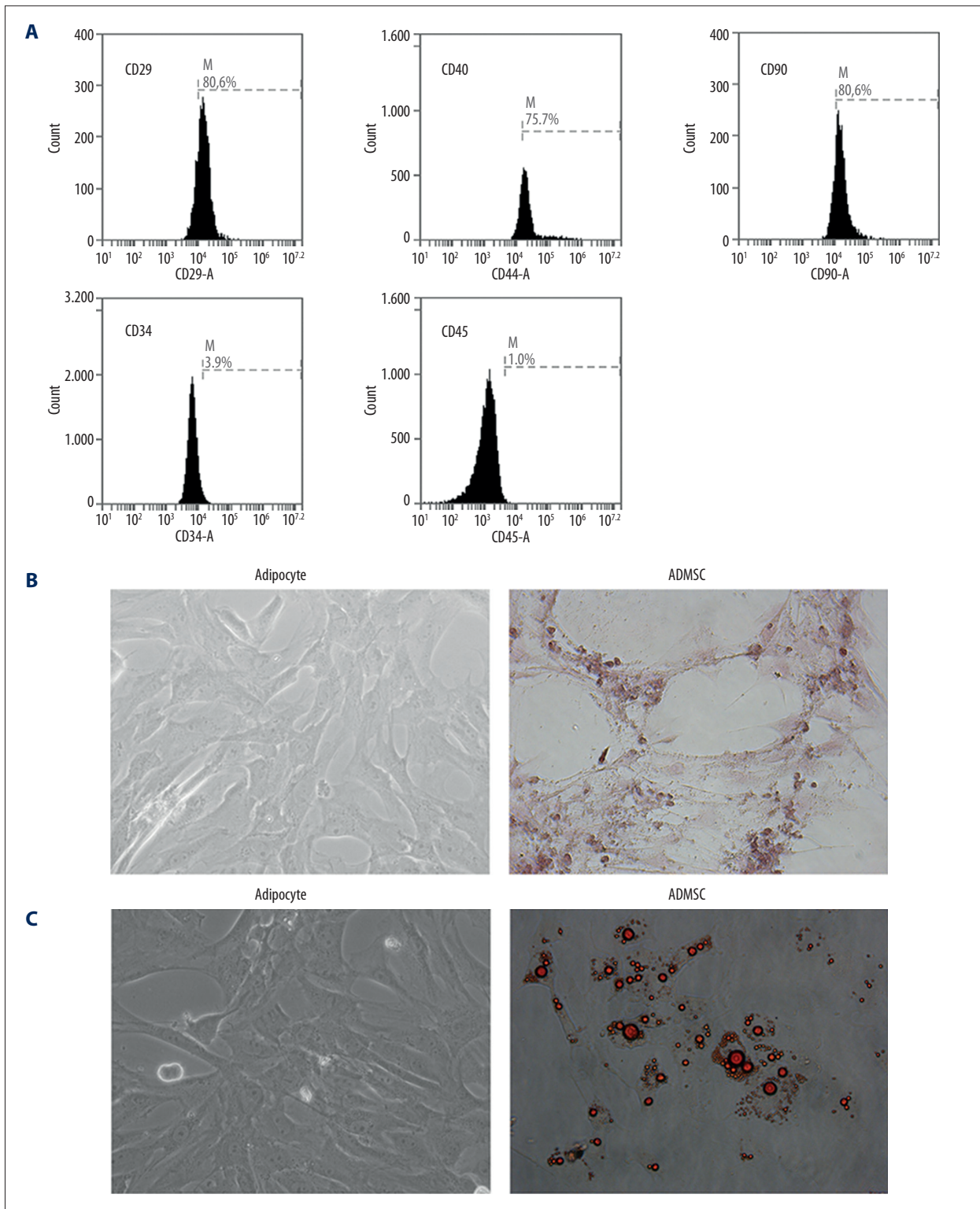


Figure 1. Identification of ADMSCs. **(A)** Flow cytometry detection of surface antigens on ADMSCs: after induction, the CD29+, CD40+, and CD90+ cells were the highest populations of stem cells. **(B)** Representative images of osteogenic differentiation of ADMSCs as detected by Alizarin Red S method; osteogenic ADMSCs were stained red. **(C)** representative images of adipogenic differentiation of ADMSCs as detected by Oil Red O method; adipogenic ADMSCs were stained red. Magnification: 400 \times .

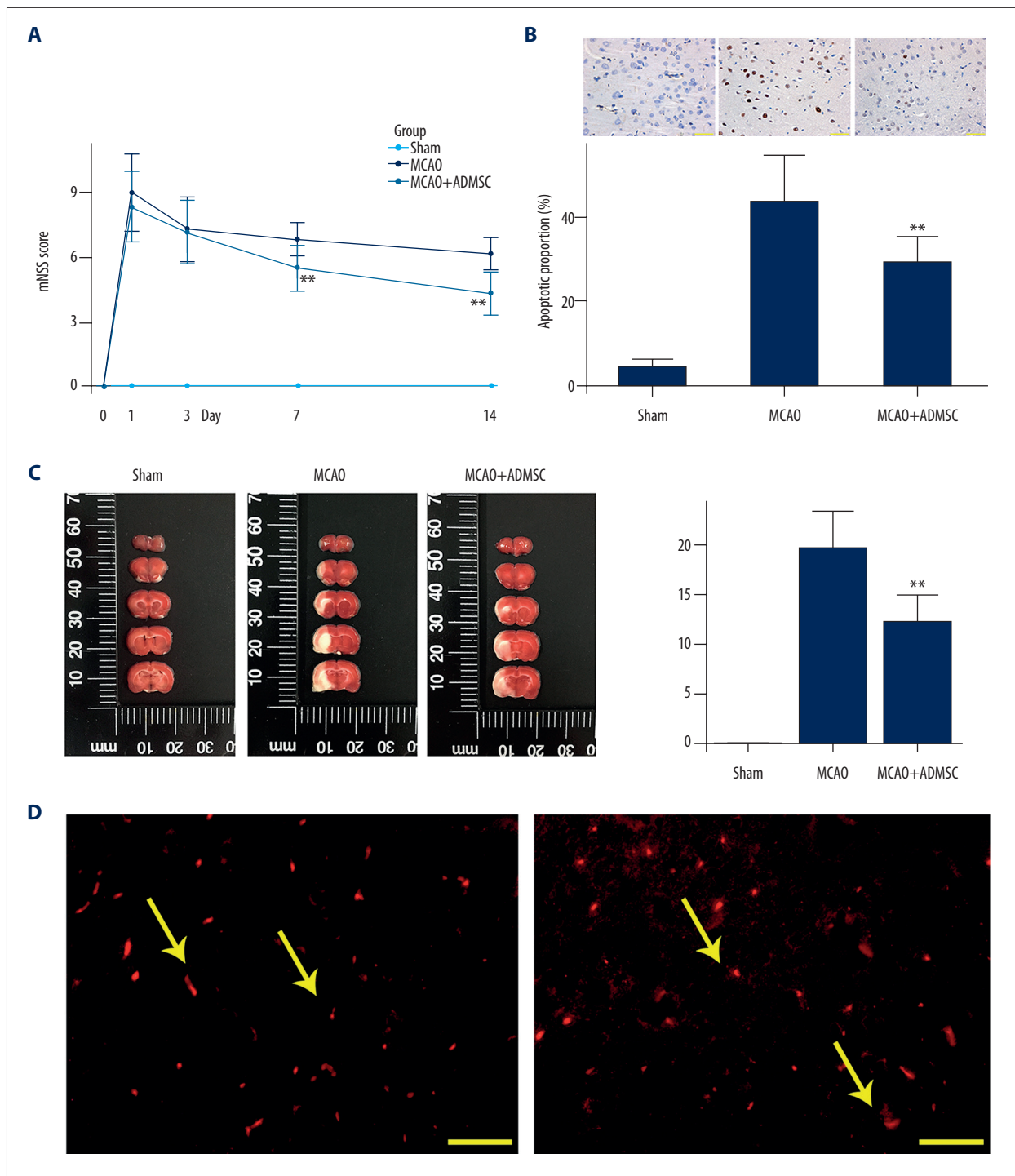


Figure 2. Administration of ADMSCs alleviated impairment of function and structure of ischemic brain. **(A)** The mNSS of rats in different groups were measured at 0, 1, 3, 7, and 14 days. The highest scores were both recorded on day 1 for the MCAO and the MCAO+ADMSC groups, and then the score gradually decreased with time. For mNSS at 7 and 14 days, values of the MCAO+ADMSC group were significantly lower than those of the MCAO group. ** $P < 0.01$ vs. the MCAO group. **(B)** representative images and quantitative analysis results of apoptosis in rat models as illustrated by TUNEL staining. Scale bar, 50 μ m. ** $P < 0.01$ vs. the MCAO group. **(C)** quantitative analysis result and representative images of TTC staining: treatment of ADMSC significantly decreased the infarct area caused by ischemia injury. ** $P < 0.01$ vs. the MCAO group. **(D)** Identification of CM-Dil-stained ADMSCs (yellow arrows) in brain ischemic penumbra area of 2 rats from the MCAO+ADMSC group. Scale bar, 50 μ m.

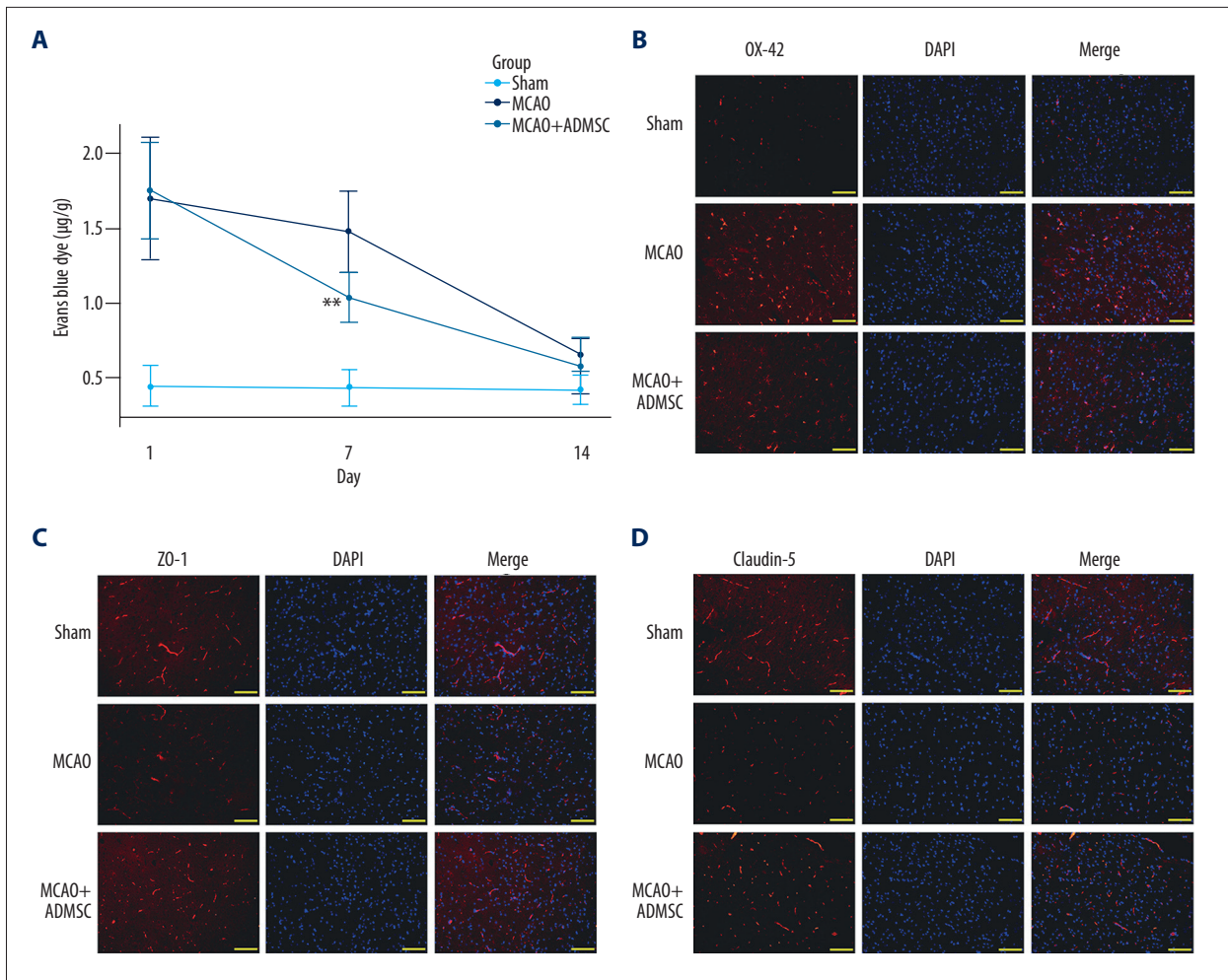


Figure 3. Administration of ADMSCs decreased permeability of BBB ischemic brains. **(A)** Results of Evans Blue dye showed that permeability of BBB decreased, even without any treatment, but administration of ADMSC accelerated the recovery process. ** $P < 0.01$ vs. the MCAO group. **(B)** representative images of immunofluorescent assay of OX-42: administration of ADMSC restricted the expression and distribution of the indicator. **(C)** representative images of immunofluorescent assay of ZO-1: administration of ADMSC increased the expression and distribution of the indicator. **(D)** representative images of immunofluorescent assay of Claudin-5: administration of ADMSC increased the expression and distribution of the indicator. Scale bar, 50 μ M.

The beneficial effect of ADMSCs on brain tissues were exerted via suppression of ER stress

ER stress is critical to both apoptotic and inflammatory processes. Therefore, the mechanism underlying the effect of ADMSCs on brain tissues was explored by focusing on its influence on ER stress-related pathways. We found that after the induction of MCAO model, the expressions of unfolded protein response (UPR) indicators, including GRP78, XBP-1, p-PERK, p-eIF2 α , and ATF-4, were all up-regulated (Figure 5). The level of the central molecule involved in the ER stress-induced apoptosis, CHOP, was also increased (Figure 5). Concomitantly, the expression of anti-apoptosis indicator Bcl-2 was suppressed while the expression of the pro-apoptosis indicator Bax was

induced (Figure 5). The administration of ADMSCs blocked the initiation of ER stress triggered by ischemia in brain tissues by reversing the expression pattern of all these indicators. The results preliminarily provide an explanation of the mechanism which drive the protective effect of ADMSCs on brain cells, as well as its function in other ischemia-related disorders.

Discussion

Findings outlined in the present study show the promising potential of ADMSCs in treating brain ischemia injury, which could also be used for IS of other organs: (1) ADMSC administration improved the brain function and limited brain infarction

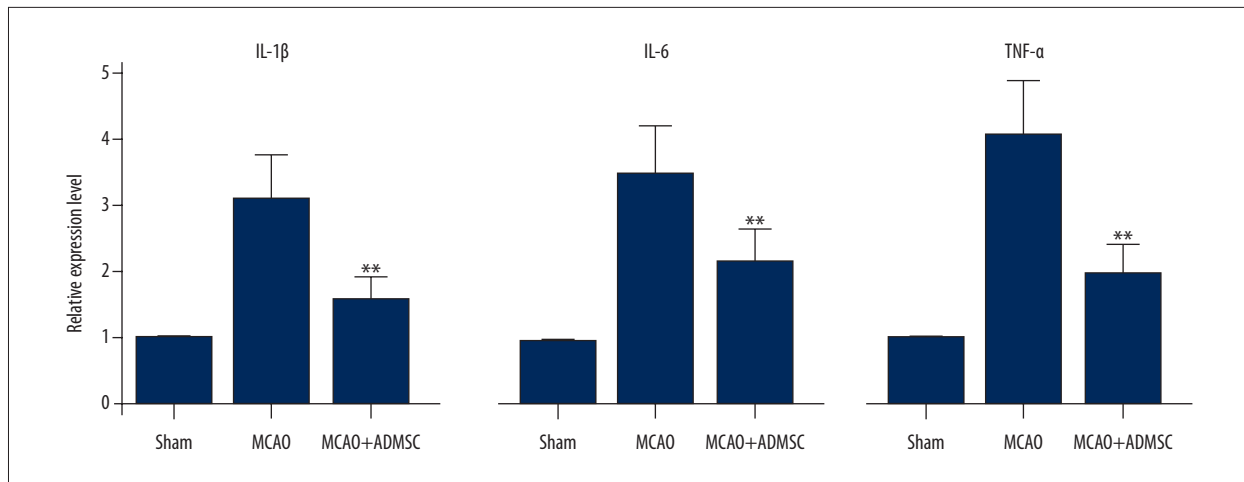


Figure 4. Administration of ADMSCs suppressed the inflammatory response in ischemic brains. After administration of ADMSCs, the production of pro-inflammation factors, including IL-1 β , IL-6, and TNF- α , were all suppressed. ** $P < 0.01$ vs. the MCAO group.

size in MCAO rats (2); ADMSC administration improved the BBB in MCAO rats; (3) ADMSC administration attenuated inflammation and apoptosis in brain infarction area; and (4) The above-mentioned effect of ADMSC therapy was attributed to its effect to suppress ischemia-induced ER stress in the brain infarction area.

Consistent with previous studies, the establishment of the MCAO model induced acute dynamic damages in brain function and structure and in the BBB [22]. The treatment with ADMSCs significantly decreased the mNSS starting on the 7th day of the experiment, which clearly indicate that ADMSC therapy improved the neural function of MCAO rats. Even without any treatment intervention, the gradual reduction of mNSS and normal reconstitution of BBB occurred at about 3 and 7 days after experimental stroke, respectively. Indeed, the brain injury inherent in stroke and other acute neurological disorders has been shown to repair itself [23], although partially. Although cerebral infarcts were healed by about 3–5 days after the IS attack, the repair of cerebral blood flow and BBB may be too slow to rescue the degenerating brain. As shown by immunofluorescent assay, the high permeability of the BBB was observed 2 weeks after MCAO model induction, which was represented by the increased level of OX-42 and decreased levels of ZO-1 and Claudin-5. Accordingly, the early return to relatively normal levels of mNSS and BBB in the ADMSC-treated MCAO animals suggests that ADMSC grafts attenuated brain alterations within the “therapeutic window” and potentially halted the pathological cascades of stroke.

Although MSCs express protein phenotypic identical to brain parenchymal cells, there is no evidence that these cells truly differentiate into and replace brain tissues. Therefore, the mechanism through which ADMSC protects the brain needs to be explored in multiple ways. The establishment of the MCAO

model also induced inflammatory responses in rat brains, which would contribute to the significant leakage across the BBB [9]. Therefore, the treatments capable of alleviating inflammation hold promise for reducing BBB permeability. In the present study, the administration of AMDSC significantly suppressed the production of all 3 pro-inflammatory factors – IL-1 β , IL-6, and TNF- α – at the mRNA level. It is well established that MSCs express anti-inflammatory cytokines like IL-10 in hematopoiesis, as well as within cerebral tissue [9]. It is the effect of these anti-inflammatory cytokines on brain tissue that contributes to the functional restoration of the brain after ADMSC treatment [24].

Compared with a previous study by Leu et al. [17], by investigating the activities of ER stress-related indicators, our study offers a preliminary explanation of the mechanism through which ADMSCs protect the brain. ER stress is characterized by the reduced protein-folding capacity of ER and is toxic to cells. Consequently, numerous pathophysiological conditions are associated with ER stress, including ischemia and neurodegenerative diseases [25,26]. The process also induces cell apoptosis through the activation of several mediators [27]. Our data show that expressions of GRP78, XBP-1, p-PERK, p-eIF2 α , ATF4, and CHOP were all up-regulated by induction of the MCAO model. With accumulation of unfolded proteins, GRP78 dissociates from the ER transmembrane receptors, leading to activation of its downstream effectors and triggering the UPR [27]. In the short-term, the UPR is a pro-survival response and restores normal ER function [28]. However, once the protein aggregation is persistent and the stress cannot be resolved, signaling switches from pro-survival to pro-apoptotic. Among the 3 transmembrane receptors, pathways related to PERK and IRE1-XBP1 are reported to induce the apoptosis. Once activated, PERK phosphorylates eIF2 α , which leads to inhibition of general (eIF2 α -dependent) protein translation and

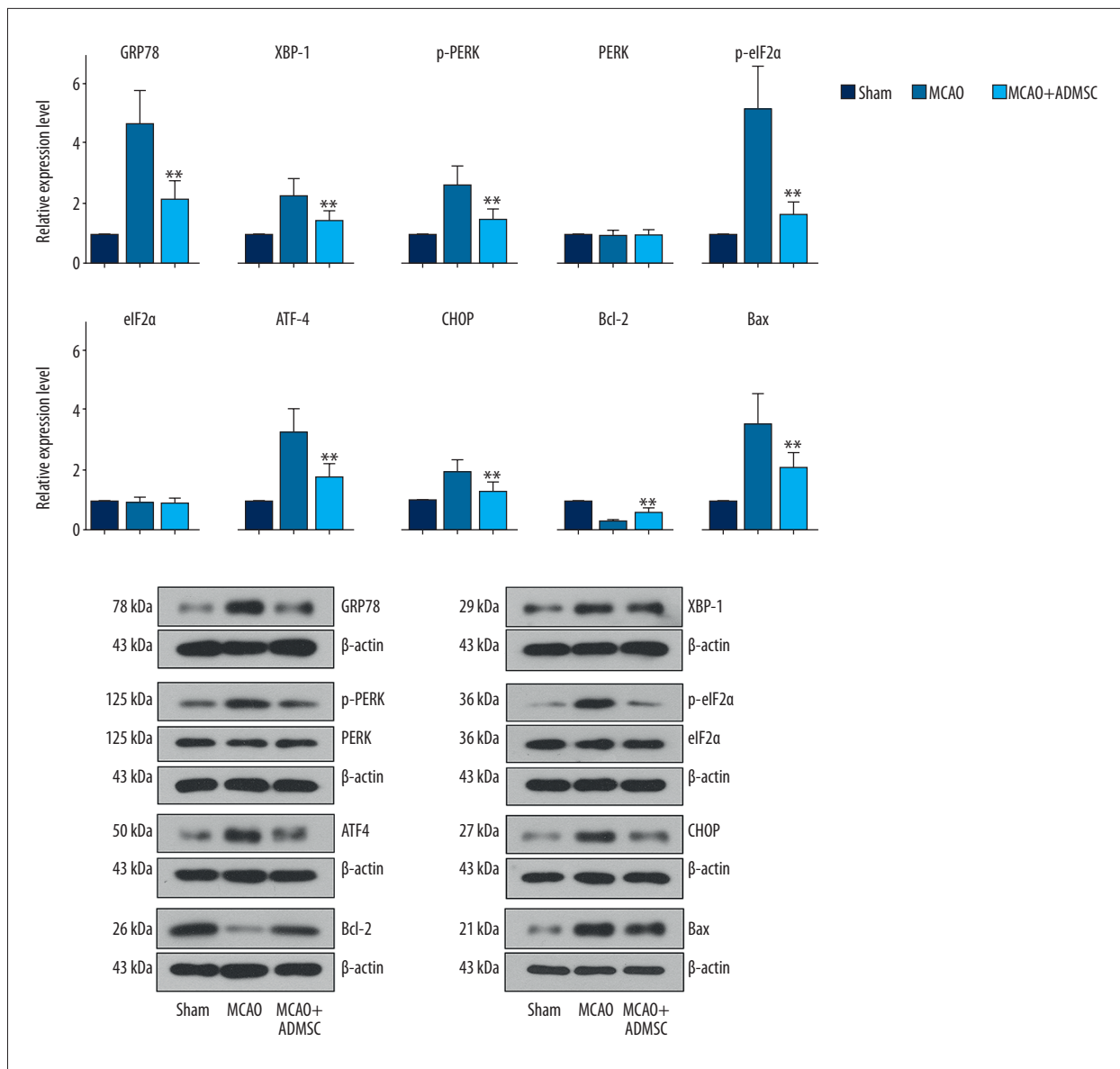


Figure 5. Administration of ADMSCs blocked the pro-apoptosis signaling induced by ER stress. After administration of ADMSCs, the expression or phosphorylation of pro-apoptosis indicators, including GRP78, XBP-1, PERK, eIF2 α , ATF4, CHOP, and Bax, were all suppressed but the expression of the anti-apoptosis indicator Bcl-2 was enhanced. ** $P < 0.01$ vs. the MCAO group.

then initiates the activity of ATF4 [29]. Although most genes induced by ATF4 are anti-apoptotic, CHOP, whose activity strongly depends on ATF4, is well known to promote apoptotic cell death [27]. In the IRE1–XBP1 axis, activated IRE1 during ER stress initially aids the UPR by splicing XBP1. At this point, either the cell returns to normal behaviors through a P58^{PK}-dependent translational inhibition relief, or if the stress persists, the IRE1–XBP1 axis triggers apoptosis by influencing the Bcl-2 family [30]. In the present study, the up-regulation of these indicators was associated with deterioration of brain function and structure. The apoptosis process in brain tissues was also verified by the decrease in the anti-apoptotic factor

Bcl-2, and increase of the pro-apoptosis factor Bax. After the administration of ADMSCs, the expression patterns of all these indicators were reversed, clearly showing the inhibition of pro-apoptosis pathways. However, the present results show that the effect of ADMSC in inducing activation of Bcl-2 was relatively weaker compared with its effect in suppressing the activity of pro-apoptosis molecules. Therefore, the therapeutic potential of ADMSC in ameliorating brain ischemia damage was mainly due to suppressing pro-apoptosis signaling rather than by inducing anti-apoptosis signaling.

Conclusions

ADMSC administration improved the neurological function, limited the brain infarct size, and suppressed the brain cell apoptosis in MCAO rats. The therapy improved brain function and BBB via its anti-inflammatory and anti-apoptosis abilities. Our

results suggest that the anti-apoptotic effect of ADMSC was through blocking ER stress-induced apoptosis. However, the course of treatments in our study was short, and more information on the long-term effect of ADMSC on IS and the prognosis after the ADMSC treatment is needed to promote the use of this therapy.

Supplementary Files

Supplementary Table 1. Detailed information of antibodies.

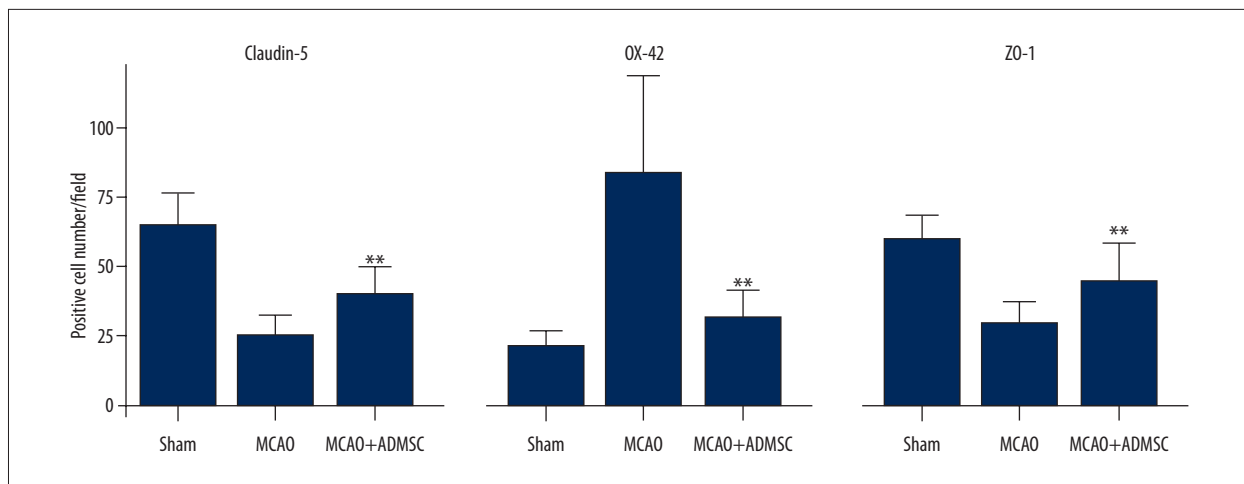
Antibody	Product	Host species	Supplier	Country	Dilution
ZO-1	21773-1-AP	Rabbit	Proteintech	CN	1: 50
Claudin-5	sc-28670	Rabbit	Santa Cruz	CN	1: 50
OX-2	ab1211	Mouse	Abcam	UK	1: 200
Cy3-labeled goat anti-rabbit IgG	A0516	Goat	Beyotime	CN	1: 200
Cy3-labeled goat anti-mouse IgG	A0521	Goat	Beyotime	CN	1: 200
GRP78	PB0669	Rabbit	BOSTER	CN	1: 400
XBP-1	PB0487	PB0487	BOSTER	CN	1: 400
p-PERK	sc-377400	Mouse	Santa Cruz	USA	1: 200
PERK antibody	sc-32577	Rabbit	Santa Cruz	USA	1: 200
p-eIF2 α	ab32157	Rabbit	Abcam	UK	1: 1000
eIF2 α	sc-11386	Rabbit	Santa Cruz	USA	1: 200
ATF4	ab184909	Rabbit	Abcam	UK	1: 1000
CHOP	#2895	Mouse	CST	CN	1: 1000
Bcl-2	bs-0032R	Rabbit	BIOSS	CN	1: 500
Bax	bs-0127R	Rabbit	BIOSS	CN	1: 500
Goat anti-rabbit IgG-HRP	A0208	Goat	Beyotime	CN	1: 5000
Goat anti-mouse IgG-HRP	A0216	Goat	Beyotime	CN	1: 5000
β -actin	sc-47778	Mouse	Santa Cruz	USA	1: 1000
CD29	11-0291-80	Armenian hamster	Ebioscience	USA	1 μ g/test
CD44	12-0444-80	Mouse	Ebioscience	USA	0.06 μ g/test
CD45	11-0461-80	Mouse	Ebioscience	USA	0.25 μ g/test
CD90	11-0900-81	Mouse	Ebioscience	USA	0.06 μ g/test
CD34	ab187284	Mouse	Abcam	UK	5 μ l/10 ⁶ cells

Supplementary Table 2. Raw data of mNSS.

Group	No. of rats	mNSS				
		0 th	1 st	3 rd	7 th	14 th
Sham	1	0	0	0	0	0
	2	0	0	0	0	0
	3	0	0	0	0	0
	4	0	0	0	0	0
	5	0	0	0	0	0
	6	0	0	0	0	0
MCAO	1	0	8	8	8	7
	2	0	6	5	6	5
	3	0	10	8	7	6
	4	0	9	6	6	7
	5	0	11	9	7	6
	6	0	10	8	7	6
MCAO+ADMSC	1	0	10	8	7	6
	2	0	10	9	5	4
	3	0	7	5	4	3
	4	0	6	6	6	5
	5	0	9	8	6	4
	6	0	8	7	5	4

Supplementary Table 3. Raw data of BBB permeability assay.

Group	No. of rats	mNSS		
		0 th	7 th	14 th
Sham	1	0.323	0.436	0.367
	2	0.589	0.409	0.551
	3	0.415	0.637	0.357
	4	0.332	0.416	0.351
	5	0.638	0.268	0.562
	6	0.406	0.469	0.384
MCAO	1	0.323	1.811	0.827
	2	0.589	1.268	0.702
	3	0.415	1.650	0.535
	4	0.332	1.060	0.540
	5	0.638	1.476	0.659
	6	0.406	1.616	0.719
MCAO+ADMSC	1	0.323	0.885	0.713
	2	0.589	1.006	0.821
	3	0.415	1.288	0.389
	4	0.332	1.026	0.692
	5	0.638	1.174	0.513
	6	0.406	0.865	0.389



Supplementary Figure 1. Quantitative analysis results of immunofluorescent detection of OX-42, ZO-1, and Claudin-5 in different groups. ** $P < 0.01$ vs. the MCAO group.

References:

- Hankey GJ: Stroke: How large a public health problem, and how can the neurologist help? *Arch Neurol*, 1999; 56(6): 748–54
- Béjot Y, Daubail B, Giroud M: Epidemiology of stroke and transient ischemic attacks: Current knowledge and perspectives. *Rev Neurol (Paris)*, 2016; 172(1): 59–68.
- Bacigaluppi M, Pluchino S, Martino G et al: Neural stem/precursor cells for the treatment of ischemic stroke. *J Neurol Sci*, 2008; 265(1): 73–77
- Favate AS, Younger DS: Epidemiology of ischemic stroke. *Neurol Clin*, 2016; 34(4): 967–80
- Kamat SG, Michelson AD, Benoit SE et al: Tissue plasminogen activator for acute ischemic stroke. *N Engl J Med*, 1996; (334): 1405–6
- Catanese L, Tarsia J, Fisher M: Acute ischemic stroke therapy overview. *Circ Res*, 2017; 120(3): 541–58
- Bravata DM: Intravenous thrombolysis in acute ischaemic stroke. *CNS Drugs*, 2005; 19(4): 295–302
- Zoppo G, Ginis I, Hallenbeck JM et al: Inflammation and stroke: Putative role for cytokines, adhesion molecules and iNOS in brain response to ischemia. *Brain Pathol*, 2000; 10(1): 95–112
- Abbott NJ: Inflammatory mediators and modulation of blood–brain barrier permeability. *Cell Mol Neurobiol*, 2000; 20(2): 131–47
- Almutairi MMA, Gong C, Xu YG et al: Factors controlling permeability of the blood–brain barrier. *Cell Mol Life Sci*, 2016; 73(1): 57–77
- Perry VH, Anthony DC, Bolton SJ et al: The blood–brain barrier and the inflammatory response. *Mol Med Today*, 1997; 3(8): 335–41
- Pittenger MF, Mackay AM, Beck SC et al: Multilineage potential of adult human mesenchymal stem cells. *Science*, 1999; 284(5411): 143–47
- Panchision DM: Concise review: Progress and challenges in using human stem cells for biological and therapeutics discovery: Neuropsychiatric disorders. *Stem Cells*, 2016; 34(3): 523–36
- Chang Y-C, Shyu W-C, Lin S-Z et al: Regenerative therapy for stroke. *Cell Transplant*, 2007; 16(2): 171–81
- Li G, Yu F, Lei T et al: Bone marrow mesenchymal stem cell therapy in ischemic stroke: Mechanisms of action and treatment optimization strategies. *Neural Regen Res*, 2016; 11(6): 1015–24
- Wan H, Li F, Zhu L et al: Update on therapeutic mechanism for bone marrow stromal cells in ischemic stroke. *J Mol Neurosci*, 2014; 52(2): 177–85
- Leu S, Lin Y-C, Yuen C-M et al: Adipose-derived mesenchymal stem cells markedly attenuate brain infarct size and improve neurological function in rats. *J Transl Med*, 2010; 8: 63
- Banas A, Teratani T, Yamamoto Y et al: IFATS collection: *In vivo* therapeutic potential of human adipose tissue mesenchymal stem cells after transplantation into mice with liver injury. *Stem Cells*, 2008; 26(10): 2705–12
- Li WY, Jin RL, Hu XY et al: Proteomic analysis of ischemic rat brain after human mesenchymal stem cell transplantation. *Tissue Engineering and Regenerative Medicine*, 2014; 11(4): 333–39
- Li F, Niyibizi C: Cells derived from murine induced pluripotent stem cells (iPSC) by treatment with members of TGF-beta family give rise to osteoblasts differentiation and form bone *in vivo*. *BMC Cell Biol*, 2012; 13: 35
- Chen J, Li Y, Wang L et al: Therapeutic benefit of intravenous administration of bone marrow stromal cells after cerebral ischemia in rats. *Stroke*, 2001; 32(4): 1005–11
- Chen W, Guo Y, Yang W et al: Protective effect of ginsenoside Rb1 on integrity of blood–brain barrier following cerebral ischemia. *Exp Brain Res*, 2015; 233(10): 2823–31
- Borlongan CV, Fujisaki T, Watanabe S: Chronic cyclosporine-A injection in rats with damaged blood–brain barrier does not impair retention of passive avoidance. *Neurosci Res*, 1998; 32(3): 195–200
- Li Y, Chen J, Chen XG et al: Human marrow stromal cell therapy for stroke in rat neurotrophins and functional recovery. *Neurology*, 2002; 59(4): 514–23
- Kaufman RJ: Orchestrating the unfolded protein response in health and disease. *J Clin Invest*, 2002; 110(10): 1389–98
- Garcia-Huerta P, Troncoso-Escudero P, Jerez C et al: The intersection between growth factors, autophagy and ER stress: A new target to treat neurodegenerative diseases? *Brain Res*, 2016; 1649: 173–80
- Szegezdi E, Logue SE, Gorman AM et al: Mediators of endoplasmic reticulum stress-induced apoptosis. *EMBO Rep*, 2006; 7(9): 880–85
- Schröder M, Kaufman RJ: The mammalian unfolded protein response. *Annu Rev Biochem*, 2005; 74: 739–89
- Harding HP, Zhang Y, Zeng H et al: An integrated stress response regulates amino acid metabolism and resistance to oxidative stress. *Mol Cell*, 2003; 11(3): 619–33
- Davis RJ: Signal transduction by the JNK group of MAP kinases. *Cell*, 2000; 103(2): 239–52